

# Signal-to-Noise Performance of Two Analog Photonic Links Using Different Noise Reduction Techniques

Edward I. Ackerman, Gary E. Betts, William K. Burns, Joseph C. Campbell<sup>(1)</sup>, Charles H. Cox, III, Ning Duan<sup>(1)</sup>, Joelle L. Prince, Michael D. Regan, and Harold V. Roussell

Photonic Systems, Inc., Billerica, MA, 01821, USA

<sup>(1)</sup>University of Virginia, Charlottesville, VA, 22904, USA

**Abstract** — We demonstrate two analog photonic links that use different noise reduction techniques to achieve high gain and low noise figure without electronic amplification. Both links use a high-power, low-noise master oscillator power amplifier as the optical source, a balanced-bridge dual-output LiNbO<sub>3</sub> Mach-Zehnder modulator with a record low  $V_{\pi} = 1.33$  V at 12 GHz, and either one or two high-power rear-illuminated photodetectors. In the first link, both outputs of the quadrature-biased modulator are used to illuminate two photodetectors configured for laser noise cancellation, yielding record high gain ( $> 17.0$  dB) and low noise figure ( $< 6.9$  dB) across the 6 – 12 GHz band. The second link uses low biasing to maximize the signal-to-noise ratio in one of the two modulator outputs, and thus requires only one photodetector. This link has lower gain ( $> 12.7$  dB) but also record low noise figure ( $< 5.7$  dB) across this same frequency band.

**Index Terms** — Optical fiber communication, laser noise, electrooptic modulation, photodetectors.

## I. INTRODUCTION

Designers of systems operating at microwave frequencies often want the benefits of using optical fiber to route their signals, but cannot tolerate having to pre-amplify the optical link by as much as 20 – 30 dB to ensure a desired signal-to-noise characteristic (i.e., noise figure).

This paper describes our efforts to design photonic links with low noise figure at useful frequencies in the C- and X-band range without any electronic amplification. To pursue this goal we first limited our design space to include only intensity-modulation/direct-detection link architectures. We further down-selected to external rather than direct modulation of the light, because external modulation of a high-power optical source with low relative intensity noise (RIN) yields higher modulation efficiency and a greater signal-to-noise ratio in the optical fiber than what can be achieved by directly modulating a semiconductor laser [1]. We then worked to maximize the performance of all three key components in the external modulation link: the optical source, the modulator, and the photodetector. We summarize these efforts in Section II. Additionally, in separate links we leveraged two different established noise figure minimization techniques: (1) balanced detection of a dual-output Mach-Zehnder modulator [2, 3] to maximize the link's output signal and suppress the laser's RIN, and; (2) operating the modulator beyond its maximum-gain quadrature bias point [4-6], which

reduces the effects of both RIN and shot noise to a greater degree than it sacrifices signal modulation efficiency. We describe these two configurations in greater detail, and report measured 6 – 12 GHz performance for both configurations, in Section III. To our knowledge this is the first time that these two configurations have been directly compared using the same set of experimental hardware.

## II. LINK COMPONENT DEVELOPMENT

### A. Optical Source

To achieve the high optical power levels necessary for the resulting link gain and noise figure, Photonic Systems, Inc. (PSI) constructed a master oscillator power amplifier (MOPA) from a 150-mW Er-doped fiber laser oscillator followed by an Er-doped fiber amplifier. This MOPA supplied a measured 3 W of 1.55- $\mu$ m optical power to its polarization-maintaining single-mode fiber pigtail. We measured the RIN of this MOPA source by tapping off a fraction of its optical output power to a calibrated detector and measuring the electrical noise power using an Agilent N8975 Noise Figure Analyzer. Between 6 and 12 GHz the measured RIN was  $-172 \pm 1$  dB/Hz, which to our knowledge is the lowest RIN measured for a laser operating at such high optical output power. In both of the link architectures described in Section III, the effect of this already low RIN is further suppressed, such that the link's noise figure is limited by a combination of thermal and shot noise.

### B. Electro-optic Modulator

The microwave performance of a Mach-Zehnder modulator-based external modulation link is dictated by the modulator's bias- and frequency-dependent slope efficiency

$$s_{mzi}(\phi, f) = \frac{\pi P_l T_{ff} R_s}{2V_{\pi}(f)} \cos \phi, \quad (1)$$

where  $P_l$  is the modulator's optical input power,  $T_{ff}$  is its fiber-to-fiber insertion loss, and  $V_{\pi}(f)$  is its frequency-dependent on-off switching voltage, as measured from the input port that's connected to the RF signal source of impedance  $R_s$  [7]. The angle  $\phi$  denotes how far the modulator is biased away from its quadrature point, which we define here as  $\phi = 0$ . It is relevant

to a discussion further on in the paper that the link's gain is proportional to  $s_{mzi}^2$  and therefore to  $\cos^2\phi$ .

Reviewing the noise figures previously reported for *intrinsic* analog photonic links (defined as links without any electronic amplifiers), we see that the large reported values of  $V_\pi(f)$  – especially at X-band and higher frequencies – exhibited by most modulators described in the literature to date has precluded demonstrations of links with better signal-to-noise performance. Neglecting both the RF reflections within the modulator and the RF-optical velocity mismatch, the frequency dependence of a traveling-wave Mach-Zehnder modulator's  $V_\pi$  has been derived previously [8]:

$$V_\pi(f) = V_\pi(DC) \frac{\alpha(f)L}{1 - e^{-\alpha(f)L}} e^{\alpha_h(f)L_h}, \quad (2)$$

where  $\alpha_h$  and  $L_h$  are the attenuation coefficient and length, respectively, of any transmission line between the modulator input and the point at which the microwave and optical fields begin to interact, and where  $\alpha$  and  $L$  apply over the region of microwave-optical interaction. The baseband term  $V_\pi(DC)$  is inversely proportional to  $L$ , and the other factors dictating its magnitude are further detailed in [8].

PSI designed a LiNbO<sub>3</sub> balanced-bridge dual-output Mach-Zehnder modulator with our primary goal being the minimization of  $V_\pi(f)$  across the 6 – 12 GHz band, which required that we minimize both  $\alpha$  and  $\alpha_h$ . Fig. 1 shows measured  $V_\pi(f)$  data points for this modulator at 1, 6, 10, and 12 GHz, along with a plot of  $V_\pi$  modeled by plugging the parameter values listed in the figure into a more complicated version of (2) that does account for impedance and velocity mismatches. To our knowledge, the measured 6, 10, and 12 GHz  $V_\pi$ 's of 1.08 V, 1.25 V, and 1.33 V are the lowest ever reported at these frequencies. The measured optical insertion loss of this modulator,  $10 \cdot \log(T_{off})$ , was approximately – 8 dB.

### C. Photodetectors

Two characteristics of a photodetector dictate its usefulness in a high-gain, low-noise figure link—its slope efficiency and its ability to perform well under high levels of illumination. In surface-illuminated photodetectors, which are easier than edge-illuminated photodetectors to manufacture, test, and couple to optical fiber, both of these qualities depend on microwave frequency in ways that make it difficult to optimize them and still achieve high-frequency operation [9]. In a surface-illuminated device large enough to support the photocurrent required for good link performance, bandwidth is typically limited by the device capacitance  $C_d$ , and therefore its frequency-dependent responsivity,  $r_d(f)$ , can be expressed as

$$r_d(f) = \frac{r_d(DC)}{1 + [2\pi f C_d (R_l + R_d)]^2}, \quad (3)$$

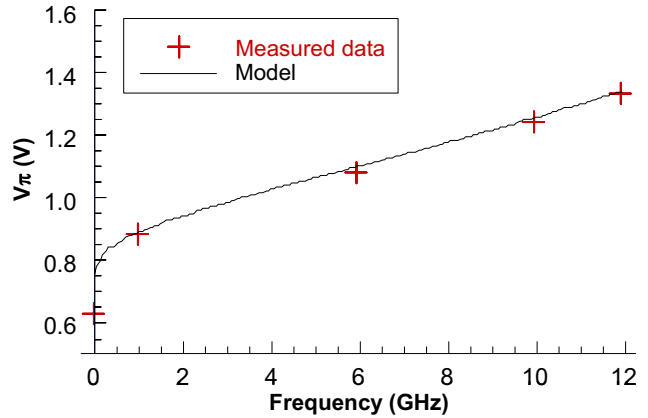


Fig. 1. Measured (red '+' symbols) vs. modeled (black curve)  $V_\pi$  of PSI's LiNbO<sub>3</sub> balanced-bridge dual-output Mach-Zehnder modulator.

where  $R_l$  is the load resistance presented to the photodetector,  $r_d(DC)$  is its static responsivity, and  $R_d$  is its series contact resistance (usually a few  $\Omega$ ). For an unpackaged device accessed via RF probes (as in our links),  $R_l$  is typically 50  $\Omega$ , whereas a packaged photodetector typically includes a back-termination resistance to optimize RF return loss and thereby typically reduces  $R_l$  to 25  $\Omega$  (the 50- $\Omega$  back termination in parallel with the usual 50- $\Omega$  load impedance).

In one of the two links we describe in Section III, high power handling was of prime importance. Motivated by this need, Professor Joe Campbell's group at University of Virginia (UVA) designed rear-illuminated photodetectors with partially depleted absorber regions, which had  $r_d \sim 1.0$  A/W at 1.55  $\mu\text{m}$ . From the measured frequency response of one device, we calculated values for  $C_d$  and  $R_d$  of  $\sim 0.15$  pF and 3  $\Omega$ , respectively. Professor Campbell plans to publish further details about these photodetectors in future journal articles.

## III. LINK CONFIGURATIONS AND EXPERIMENTAL RESULTS

### A. Balanced Detection of Two Outputs from a Balanced-Bridge Mach-Zehnder Modulator

The first link we assembled using the high-power, low-RIN MOPA and low- $V_\pi$  balanced-bridge modulator used a chip fabricated by UVA with two photodetectors in a differential configuration. This link configuration is shown in Fig. 2(A).

The photodetectors' power handling capability allowed us to use about 1.5 W of the laser's output optical power when the modulator was quadrature-biased ( $\phi = 0$ ). The modulator's two optical outputs were routed to the two devices on the balanced photodetector chip via optical fibers whose length we matched to one another as precisely as possible. We also attempted to equalize the two photocurrent magnitudes. At  $\phi = 0$ , both average photocurrents were measured at  $\sim 80$  mA.

The blue curves plotted in Fig. 3 show the gain and noise figure of the link diagrammed in Fig. 2(A) at frequencies

between 6 and 12 GHz, which we measured using an Agilent N8975A Noise Figure Analyzer. At 6 GHz the measured gain was  $> 24.2$  dB, which rolled off to a gain of just over 17.0 dB at 12 GHz due to the frequency responses of the modulator and balanced photodetectors. Because the balanced photodetector circuit situates two of the devices in parallel with one another, the effective  $C_d$  is twice that of a single device, or  $\sim 0.3$  pF. Regardless, to our knowledge this result is the highest photonic link gain that has been demonstrated in the 6 – 12 GHz range without using any amplifiers.

Because the two modulated outputs of the balanced-bridge modulator are  $180^\circ$  out of phase with one another, subtracting them in the differential photodetector circuit doubles output signal current (which increases the link gain) while cancelling the common-mode component. For perfect balance, this common mode is the RIN of the MOPA. We have shown that all of this extra effort – i.e., using two photodetectors and taking great pains to balance the signals in the two optical fiber paths that connect them to the two outputs of the modulator – yields excellent gain and noise figure. Additionally, because the modulator is operated at quadrature, second-order distortion is minimized, so that the link’s broadband spurious-free dynamic range (SFDR) is limited only by 3<sup>rd</sup>-order rather than by 2<sup>nd</sup>-order distortion. This is this link configuration’s main benefit, as we show in row A of Table I. Also listed in that row are some disadvantages associated with this approach, including the fact that operation at quadrature bias results in high optical powers in both of the optical fibers and at both photodetectors. High power can limit the transmission distance in fiber because of Stimulated Brillouin Scattering (SBS) [10], and high optical power at the photodetectors can limit the link’s SFDR.

### B. Detection of a Single Output of the Modulator at Low Bias

The second link we built used the same laser, but used only one of the same modulator’s two output fibers; the modulator was biased for low average optical power in this fiber. We coupled this fiber’s output onto a single UVA photodetector. This link configuration is shown in Fig. 2(B).

The key benefit of low-biasing is that, for large enough modulator input optical power  $P_I$ , a link’s output signal-to-noise ratio actually *increases* as the modulator is biased away from quadrature towards its lowest-output bias point. This occurs because the shot noise generated in a photodetector is proportional to the average optical power, and this power is proportional to the factor  $(1 - \sin \phi)$ , which decreases even faster with increasing  $\phi$  than  $s_{mzi}$  does. Additionally, the link’s output noise due to laser RIN is proportional to  $(1 - \sin \phi)^2$ , which decreases with increasing  $\phi$  even faster than the shot noise. At some value of  $\phi$ , however, the shot noise decreases to a magnitude smaller than that of the thermal noise from the detector load resistor ( $-174$  dBm/Hz at  $T = 290$  K), and thus further increasing  $\phi$  degrades signal-to-noise ratio. Therefore, for any  $P_I$  there is a corresponding optimum value of  $\phi$  [6].

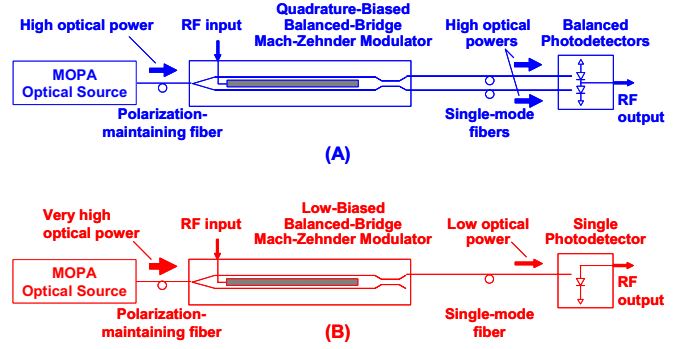


Fig. 2. Analog photonic link configurations with noise reduction. In configuration (A), equal-length fibers convey two equal-magnitude,  $180^\circ$  out-of-phase outputs from the balanced-bridge Mach-Zehnder modulator to a pair of balanced photodetectors. Noise reduction in configuration (B) is achieved using the established low biasing technique [4-6].

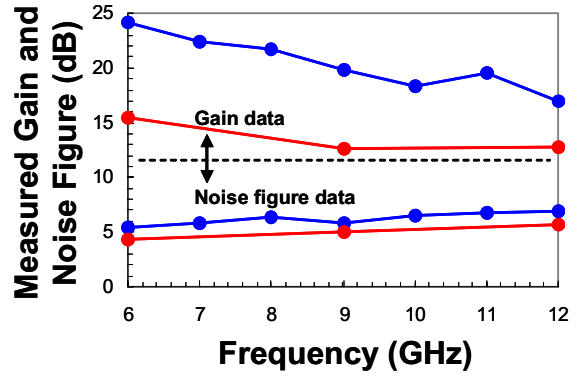


Fig. 3. Measured gain and noise figure of links using (A) balanced photodetectors to differentially detect two anti-phase-modulated outputs of a Mach-Zehnder modulator (blue curves), and (B) a single photodetector to detect one output of a low-biased Mach-Zehnder modulator (red curves).

As has been previously reported [6], we discovered that noise figure comparable to that enabled by configuration A can be achieved using this low-biasing configuration B *only if you use even greater  $P_I$  than we used in configuration A*. Using models based on those published in [1] and [7], we determined that noise figure  $< 6$  dB could be achieved across 6 – 12 GHz if we used 2.5 W of the MOPA’s output power and biased the modulator at  $\phi = 75^\circ$ . The red circles in Fig. 3 show the measured link gain and noise figure of link configuration B under these conditions. To our knowledge, our value of  $P_I = 2.5$  W of input power is the largest input power ever tolerated by a high-speed optical modulator of any variety. As of this writing, we have only subjected one of PSI’s modulators to brief durations (less than one minute) of  $P_I = 2.5$  W. We have, however, run another one of PSI’s modulators for 24 hours at a constant 1.75 W with no observable change in  $T_{ff}$  and no significant bias drift.

TABLE I  
COMPARISON OF THE TWO NOISE-REDUCTION LINK ARCHITECTURES DIAGRAMMED IN FIG. 2

Configuration	Principal Benefit	Relative Disadvantages
<b>A. Balanced detection</b>	SFDR is limited by 3 <sup>rd</sup> -order (rather than 2 <sup>nd</sup> -order) distortion over multi-octave bandwidths	<ul style="list-style-type: none"> <li>• High optical power in the fibers connecting the modulator to the detectors causes an SBS-imposed limit on link length</li> <li>• Two photodetectors and fiber spans are required</li> <li>• Precise amplitude and phase balance must be maintained in the two long paths from modulator outputs to detectors</li> <li>• Photodetectors receive high optical power, and thus impose limit on SFDR unless they are large, which then limits their bandwidth</li> <li>• R-C response of two photodetectors in parallel imparts worse roll-off to the link's gain vs. frequency (especially if they're large)</li> </ul>
<b>B. Low biasing</b>	Single fiber and single photodetector need withstand only modest optical powers	<ul style="list-style-type: none"> <li>• To achieve noise figure comparable to that of a balanced-detector link requires even greater optical power into the modulator; SBS therefore limits distance between laser and modulator</li> <li>• Away from quadrature bias, modulator generates strong 2<sup>nd</sup>-order distortion products, limiting link bandwidth to &lt; one octave</li> </ul>

As shown in row B of Table I, the chief advantage of the low biasing approach is its simplicity. Additionally, the average photodetector current we measured when operating the laser at 2.5 W of output power and the modulator at  $\phi = 75^\circ$  was only 6.2 mA. Compared to the quadrature bias case, then, in general achieving similar noise figures using a low-biasing configuration requires the laser to generate – and the modulator to withstand – greater optical power, but requires the optical fiber and photodetector to withstand less power. One consequence of this shift in the link's optical power distribution is that it further reduces the SBS-limited distance between the laser and modulator, but increases the SBS-limited distance by which the modulator and photodetector can be separated. Finally, as shown in Table I, a distinct disadvantage of biasing the modulator away from quadrature is that it results in strong generation of second-order distortion, thereby limiting the operational bandwidth of any system using such a link to one octave or narrower.

#### IV. SUMMARY

We have demonstrated and for the first time compared two previously established configurations for reducing the noise figure of an analog photonic link. In our experimental investigation of both link configurations, we used the same laser, modulator, and photodetector components, which we had engineered for high performance in the 6 – 12 GHz band. One link we built, which was suitable for multi-octave bandwidth operation, demonstrated a noise figure of < 6.9 dB and a gain of > 17.0 dB across 6 – 12 GHz. Record low noise figure results were measured (4.4 dB at 6 GHz and < 5.7 dB across the 6 – 12 GHz band, with a link gain of > 12.7 dB across this band) using a second configuration that included a low-biased Mach-Zehnder modulator; this link is suitable for operation across frequency bands up to one octave in width.

#### ACKNOWLEDGEMENT

This material is based upon work supported by DARPA under SSC-San Diego Contract No. N66001-04-C-8045. Any opinions, findings and conclusions or recommendations expressed in this material are those of the authors and do not necessarily reflect the views of DARPA or SSC San Diego.

#### REFERENCES

- [1] C. Cox, E. Ackerman, G. Betts, and J. Prince, "Limits on the performance of RF-over-fiber links and their impact on device design," *IEEE Trans. Microwave Theory & Tech.*, vol. 54, no. 2, pp. 906-920, Feb. 2006.
- [2] E. Ackerman, S. Wanuga, J. MacDonald, and J. Prince, "Balanced receiver external modulation fiber-optic link architecture with reduced noise figure," *1993 IEEE MTT-S Int. Microwave Symp. Dig.*, vol. 2, pp. 723-726, Jun. 1993.
- [3] K. Williams, L. Nichols, and R. Esman, "Externally-modulated 3 GHz fiber-optic link utilizing high current and balanced detection," *Electron. Lett.*, vol. 33, pp. 1327-1328, Jul. 1997.
- [4] G. Betts and F. O'Donnell, "Improvements in passive, low-noise-figure optical links," *Proc. Photonic Systems for Antenna Applications Conf.* (Monterey), pp. 41-43, 1993.
- [5] M. Farwell, W. Chang, and D. Huber, "Increased linear dynamic range by low biasing the Mach-Zehnder modulator," *IEEE Photon. Technol. Lett.*, vol. 5, pp. 779-782, Jul. 1993.
- [6] E. Ackerman, S. Wanuga, D. Kasemset, A. Daryoush, and N. Samant, "Maximum dynamic range operation of a microwave external modulation fiber-optic link," *IEEE Trans. Microwave Theory & Tech.*, vol. 41, no. 8, pp. 1299-1306, Aug. 1993.
- [7] C. Cox, *Analog Optical Links*. Cambridge Univ. Press, 2004.
- [8] G. Gopalakrishnan, W. Burns, R. McElhanon, C. Bulmer, and A. Greenblatt, "Performance and modeling of broadband LiNbO<sub>3</sub> traveling-wave optical intensity modulators," *J. Lightwave Technol.*, vol. 12, no. 10, pp. 1807-1819, Oct. 1994.
- [9] K. Williams, D. Tulchinsky, X. Li, N. Li, J. Campbell, "High-power photodiodes," *LEOS Newsletter*, p.16, Apr. 2006.
- [10] A. Chraplyvy, "Limitations on lightwave communications imposed by optical-fiber nonlinearities," *J. Lightwave Technol.*, vol. 8, pp. 1548-1557, Oct. 1990.